THE FASEB JOURNAL • RESEARCH • www.fasebj.org

KDM2B is a histone H3K79 demethylase and induces transcriptional repression *via* sirtuin-1–mediated chromatin silencing

Joo-Young Kang,* Ji-Young Kim,* Kee-Beom Kim,* Jin Woo Park,* Hana Cho,* Ja Young Hahm,* Yun-Cheol Chae,* Daehwan Kim,* Hyun Kook,[†,§] Sangmyeong Rhee,* Nam-Chul Ha,[‡] and Sang-Beom Seo*[,1]

*Department of Life Science, College of Natural Sciences, Chung-Ang University, Seoul, South Korea; [†]Department of Pharmacology, Medical Research Center for Gene Regulation, Chonnam National University, Gwangju, South Korea; and [‡]Department of Food and Animal Biotechnology, [§]Department of Agricultural Biotechnology, Seoul National University, Seoul, South Korea

ABSTRACT: The methylation of histone H3 lysine 79 (H3K79) is an active chromatin marker and is prominent in actively transcribed regions of the genome; however, demethylase of H3K79 remains unknown despite intensive research. Here, we show that KDM2B, also known as FBXL10 and a member of the Jumonji C family of proteins known for its histone H3K36 demethylase activity, is a di- and trimethyl H3K79 demethylase. We demonstrate that KDM2B induces transcriptional repression of *HOXA7* and *MEIS1 via* occupancy of promoters and demethylation of H3K79. Furthermore, genome-wide analysis suggests that H3K79 methylation levels increase when KDM2B is depleted, which indicates that KDM2B functions as an H3K79 demethylase *in vivo*. Finally, stable KDM2B-knockdown cell lines exhibit displacement of NAD^+-dependent deacetylase sirtuin-1 (SIRT1) from chromatin, with concomitant increases in H3K79 methylation and H4K16 acetylation. Our findings identify KDM2B as an H3K79 demethylase and link its function to transcriptional repression *via* SIRT1-mediated chromatin silencing.—Kang, J.-Y., Kim, J.-Y., Kim, K.-B., Park, J. W., Cho, H., Hahm, J. Y., Chae, Y.-C., Kim, D., Kook, H., Rhee, S., Ha, N.-C., Seo, S.-B. KDM2B is a histone H3K79 demethylase and induces transcriptional repression *via* sirtuin-1–mediated chromatin silencing. FASEB J. 32, 5737–5750 (2018). www.fasebj.org

KEY WORDS: histone demethylase · H3K79 methylation · SIRT1 · transcription

Chromatin structure is modulated by diverse covalent histone modifications (1, 2). Combinations of such modifications direct both global and specific transcriptional outcomes (3, 4). Among these modifications, histone lysine methylation is linked to both the activation and repression of transcription. As in the case of most epigenetic modifications, histone methylation and demethylation are dynamically regulated by histone methyltransferases (HMTases) and demethylases (5–7).

Histone H3 lysine 79 methylation (H3K79me) is catalyzed by the HMTase disruptor of telomeric silencing-1 (Dot1)–like (DOT1L), which is the mammalian homolog of the yeast, Dot1 (8–11). DOT1L is considered the only H3K79 HMTase in mammals; however, recent reports suggest that the nuclear SET [Su(var)3-9, Enhancer-of-zeste, Trithorax] domain (NSD) family of HMTases, including response element II binding protein (also known as NSD2), has H3K79-methylating activities (12, 13). On the basis of analyses of its crystal structure, H3K79 is a surface-exposed residue and is located in proximity to lysine 123 of histone H2B in yeast cells (14, 15). Regulation occurs by *trans*-crosstalk, and ubiquitylation of histone H2BK123 (H2BK123ub1) is necessary for H3K79me formation (16).

H3K79me is linked to active gene transcription (17–21). In addition, ubiquitylation of histone H2BK123 (H2BK123ub1), H3K4me, H3K79me, and RNA polymerase II phosphorylation occurs sequentially during transcriptional elongation (22). H3K79me plays a role in DNA repair *via* interaction with Rad9/53BP1, and levels of

ABBREVIATIONS: BCOR, BCL6 corepressor; CBX8, chromobox homolog 8; CDS, coding sequence; ChIP-seq, chromatin immunoprecipitation sequencing; CID, collision-induced dissociation; Dot1, disruptor of telomeric silencing-1; DOT1L, disruptor of telomeric silencing-1–like; FDH, formaldehyde dehydrogenase; GST, glutathione *S*-transferase; H2BK123ub1, ubiquitylation of histone H2AK123; H3K79, histone H3 lysine 79; H3K79me, histone H3 lysine 79 methylation; HMTase, histone methyltransferase; ID, internal diameter; IP, immunoprecipitation; JmjC, Jumonji C; LC-MS/MS, liquid chromatography–tandem mass spectrometry; LTQ, linear trap quadropole; MLA, methyl-lysine analog; MLL, mixed lineage leukemia; MMSET, multiple myeloma set domain; PcG, polycomb group; PRC1, polycomb-repressive complex 1; qPCR, quantitative PCR; shRNA, short hairpin RNA; SIRT1, sirtuin-1; SMYD3, SET and MYND domain containing-protein 3

[1] Correspondence: Department of Life Science, College of Natural Sciences, Chung-Ang University, 221 Heukseok-dong, Dongjak-gu, Seoul 156-756, South Korea. E-mail: sangbs@cau.ac.kr

doi: 10.1096/fj.201800242R

This article includes supplemental data. Please visit *http://www.fasebj.org* to obtain this information.

H3K79me change during the cell cycle (8, 23–25). During embryogenesis, H3K79me regulates the expression of developmental genes (26, 27). In addition, aberrant hypermethylation of H3K79 results in the activation of oncogenes and leukemic transformation (28–30).

The Jumonji C (JmjC) domain–containing histone demethylase, KDM2B, also known as FBXL10, preferentially demethylates both H3K36me2/3 and H3K4me3 (31–33). KDM2B also mediates the monoubiquitylation of the histone H2AK119 as a component of noncanonical polycomb-repressive complex 1 (PRC1) in embryonic stem cells (34, 35). KDM2B enhances the reprogramming of embryonic stem cells by binding to unmethylated CpG sites *via* the zinc finger-CXXC motif. CpG recognition and PRC1 targeting by KDM2B are important for the deposition of H2AK119ub1 and for additional recruitment of PRC2 to a subset of CpG islands, which is an activity limited to variant PRC1 complexes (36–38).

KDM2B contributes to the development of tumors *in vivo*, likely *via* H3K36 demethylase activity. Overexpression of KDM2B inhibits cellular senescence by repressing the mouse loci $p16^{Ink4a}$, $p19^{Arf}$, and $p15^{Ink4b}$, and the human loci, retinoblastoma and p53, which results in cellular immortalization (39, 40). In addition, wild-type KDM2B, but not a mutant with defective demethylase activity, enhances the progression of pancreatic cancer in a mouse model (41). Furthermore, H3K36 demethylase activity is required for leukemic transformation in a Hoxa9/Meis1-induced mouse bone marrow transplantation model (42).

In the current study, we identified KDM2B as a histone demethylase that can catalyze the removal of di- and trimethyl groups from the H3K79 residue. We also found that KDM2B induces sirtuin-1 (SIRT1)–mediated chromatin silencing by removing H3K79me, which leads to transcriptional repression.

MATERIALS AND METHODS

Peptide pull-down assay

Biotinylated dimethyl H3K79 peptides, H-RLVREIAQDFK(me2)TDLRFQSSAVK(biotin)-OH, and unmodified H3K79 peptides, H-RLVREIAQDFKTDLRFQSSAVK(biotin)-OH, were purchased from AnaSpec (Fremont, CA, USA). Peptides (5 μg) were prebound to streptavidin-Sepharose beads (GE Healthcare, Waukesha, WI, USA) and incubated overnight at 4°C with nuclear extract from K562 cells, dialyzed against dialysis buffer (20 mM HEPES, pH 7.9, 1.5 mM $MgCl_2$, 20% glycerol, 0.2 mM EDTA, 100 mM KCl, and 0.5 mM DTT), and precleared. Supernatant was stored and particles were washed 5 times with 1 ml of washing buffer (20 mM HEPES, pH 7.9, 1.5 mM $MgCl_2$, 20% glycerol, 0.2 mM EDTA, 100 mM KCl, 0.5 mM DTT, and 0.1% Triton X-100). Peptide-binding proteins were separated by SDS-PAGE. A portion of them was stained with silver and the rest was divided into 3 parts to be analyzed by liquid chromatography–tandem mass spectrometry (LC-MS/MS).

Stable knockdown cell lines

DNA oligonucleotides that encode KDM2B short hairpin RNA (shRNA) #1 (5′-CTGAACCACTGCAAGTCTATC-3′) and KDM2B shRNA #2 (5′-CGGCCTTTACAAGAAGACATT-3′) were subcloned into the pLKO.1-puro lentiviral vector (Addgene, Cambridge, MA, USA), according to standard procedures. To produce virus particles, 293T cells were cotransfected with plasmids that encode vesicular stomatitis virus glycoprotein, NL-BH, and shRNAs. Two days after transfection, supernatants that contained viruses were collected and used to infect 293T cells in the presence of polybrene (8 μg/ml). After lentiviral infection of 293T cells, addition of puromycin (1 μg/ml) selected for cells that stably expressed shRNAs of KDM2B.

In vitro histone demethylase assay

Bulk histones (MilliporeSigma, Burlington, MA, USA), nucleosomes that were extracted from 293T cells, and methyl lysine analog (MLA) that contained recombinant H3K79me3 histones (Active Motif, Carlsbad, CA, USA) (43, 44) were incubated with purified glutathione *S*-transferase (GST), GST-$KDM2B_{1–734}$, or GST-KDM2B (H242A) overnight at 37°C in demethylation assay buffer (20 mM Tris-HCl, pH 7.3, 150 mM NaCl, 1 mM α-ketoglutarate, 50 μM $FeSO_4$, and 2 mM ascorbic acid).

Formaldehyde dehydrogenase assay

Formaldehyde formation was measured by spectrophotometric assay (45) using formaldehyde dehydrogenase (FDH). GST-KDM2B and MLA histone H3K79me3 were first incubated for 3 h at 37°C in demethylation assay buffer. Reaction solution was immediately mixed in buffer that contained 50 mM potassium phosphate (pH 7.2), 2 mM NAD^+, and 0.1 U FDH. FDH reaction was initiated and absorbance at 340 nm was recorded for 5 min. Absorbance at 340 nm ($\varepsilon^{340} = 6.22\ mM^{-1}\ cm^{-1}$ for NADH) was measured at each time point in a 0.5-min interval using WPA Lightwave S2000 UV/Vis spectrophotometer (Scinteck Instruments, Irvine, CA, USA). The optical density 340-nm absorbance at the moment of the addition of FDH was considered as 0 and this was used as the 0-min time point. Data were analyzed using the Excel program (Microsoft, Redmond, WA, USA).

DNA constructs

EFplink2-FLAG-KDM2B was acquired. The full-length KDM2B coding sequence (CDS) was transferred into p3XFLAG-CMV-10, and a catalytic mutant construct was generated by H242A point mutation. Regions (1–734 aa) that contained the JmjC, CXXC zinc finger, and plant homeodomain of wild-type and H242A mutant KDM2B were cloned into pGEX-4T1 for protein purification. pECE-FLAG-SIRT1 was purchased from Addgene. SIRT1 CDS was subcloned into the modified pcDNA6-hemagglutinin-MYC-HIS (Thermo Fisher Scientific, Waltham, MA, USA).

Cell culture

K562 cells were grown in RPMI 1640 medium. 293T cells were grown in DMEM that contained 10% heat-inactivated fetal bovine serum and 0.05% penicillin-streptomycin at 37°C in a 5% CO_2 atmosphere. Sirtinol (50 μM; MilliporeSigma) was treated for 2 h. PRT4165 (100 μM; Tocris Bioscience, Bristol, United Kingdom) was treated for 2 h in serum-free medium.

In-gel protein digestion and LC-MS/MS

Mass spectrometry and proteomic analyses were carried out at the Korea Basic Science Institute (Ochang Headquarters, Division of Bioconvergence Analysis). Proteins separated by 2-dimensional gel

electrophoreses were visualized using the PlusOne Silver Staining Kit (Amersham Biosciences, Little Chalfont, United Kingdom), according to the manufacturer's protocol. After electrical scanning and analysis of silver-stained gels using Phoretix Expression software (v.2005; Nonlinear Dynamics, Newcastle-upon-Tyne, United Kingdom), protein bands of interest were excised and digested in-gel with sequencing-grade modified trypsin (Promega, Madison, WI, USA). In brief, excised protein bands were washed with a 1:1 mixture of acetonitrile and 25 mM ammonium bicarbonate (pH 7.8), and subsequently dried using a SpeedVac concentrator (Thermo Fisher Scientific). After drying, rehydration was performed with 25 mM ammonium bicarbonate (pH 7.8) and trypsin. Tryptic peptides were extracted from supernatants with a 50% aqueous acetonitrile solution that contained 0.1% formic acid. After preparation, tryptic peptides were analyzed using reversed-phase capillary high-performance liquid chromatography directly coupled to a Finnigan LCQ ion trap mass spectrometer. Three extractions were performed to recover all tryptic peptides from gel slices. Recovered peptides were concentrated by drying the combined extracts in a vacuum centrifuge. Concentrated peptides were mixed with 20 μl of 0.1% formic acid in 3% acetonitrile. Nano–liquid chromatography of the tryptic peptides was performed using the Waters Nano Liquid Chromatography System (Waters, Milford, MA, USA) equipped with a Waters C18 NanoAcquity Ultra Performance Liquid Chromatography (UPLC) Column (75 μm × 15 cm). Binary solvent A1 contained 0.1% formic acid in water, and binary solvent B1 contained 0.1% formic acid in acetonitrile. Samples (5 μl) were loaded onto the column, and peptides were subsequently eluted with a binary solvent B1 gradient (2–40%, 30 min, 0.4 μl/min). The lock mass, [Glu1] fibrinopeptide at 400 fM/μl, was delivered from the auxiliary pump of the nano–liquid chromatography system at 0.3 μl/min to the reference sprayer of the NanoLockSpray source.

Nano–liquid chromatography linear trap quadropole Orbitrap elite analysis

Digested plasma samples were dissolved in mobile phase A and analyzed using an LC-MS/MS system that consisted of a Nano Acquity UPLC System (Waters) and a linear trap quadropole (LTQ) Orbitrap Elite Mass Spectrometer (Thermo Fisher Scientific) equipped with a nanoelectrospray source. An autosampler was used to load 5-μl aliquots of peptide solutions into a C18 trap column with an internal diameter (ID) 180 μm, length 20 mm, and particle size of 5 μm (Waters). Peptides were desalted and concentrated on the trap column for 10 min at a flow rate of 5 μl/min. Trapped peptides were then back-flushed and separated on a homemade microcapillary C18 column of ID 100 μm and length 200 mm (Aqua; particle size, 3 μm; 125 Å). Mobile phases were composed of 100% water (A) and 100% acetonitrile (B), each of which contained 0.1% formic acid. The liquid chromatography gradient began with 5% mobile phase B and was maintained for 15 min. Mobile phase B was linearly ramped to 15% for 5 min, 50% for 75 min, and 95% for 1 min. Then, 95% mobile phase B was maintained for 13 min before decreasing to 5% for another 1 min. The column was re-equilibrated with 5% mobile phase B for 10 min before the next run. Voltage applied to produce the electrospray was 2.2 kV. During the chromatographic separation, LTQ Orbitrap Elite was operated in data-dependent mode. MS data were acquired using the following parameters: full scans were acquired in the Orbitrap at a resolution of 120,000 for each sample; 6 data-dependent collision-induced dissociation (CID) MS/MS scans were acquired per full scan; CID scans were acquired in an LTQ with 10-ms activation times performed for each sample; 35% normalized collision energy was used in CID; and a 2-Da isolation window for MS/MS fragmentation was applied. Previously fragmented ions were excluded for 180 s. LC-MS/MS was performed using Nano Liquid Chromatography LTQ Orbitrap Elite mass spectrometry at the Korea Basic Science Institute.

Isothermal titration calorimetry

Isothermal titration calorimetry experiment was carried out using an Auto-iTC200 Microcalorimeter at the Korea Basic Science Institute. Trimethyl H3K79 peptides, AQDFK(me3)TDLR, and unmodified H3K79 peptides, AQDFKTDLR, were purchased from AnyGen (Gwangju, South Korea). The protein, GST-KDM2B, was purified and prepared in the sample cell, and the ligand (H3K79me3 peptide or H3K79me0 peptide) was loaded into the injectable syringe. All samples were prepared in 1× PBS. Titration measurements that consisted of 19 injections (2 μl) with 150-s spacing were performed at 25°C, and the syringe was stirred at 700 rpm. Data were analyzed using the MicroCal Origin software (OriginLab, Northampton, MA, USA).

Abs

Abs used in this study were as follows: anti-KDM2B (MilliporeSigma), anti-SIRT1 (MilliporeSigma), anti-DOT1L (Santa Cruz Biotechnology, Dallas, TX, USA), anti–β-actin (Santa Cruz Biotechnology), anti-FLAG (Sigma-Aldrich), anti-hemagglutinin (Santa Cruz Biotechnology), anti-H3K79me3 (Abcam, Cambridge, MA, USA), anti-H3K79me2 (Abcam), anti-H3K79me1 (Abcam), anti-H3K36me2 (Abcam), anti-H3K36me3 (Upstate, Mount Upton, NY, USA), anti-H3K4me3 (Abcam), anti-H3K9me2 (MilliporeSigma), anti-H3K27me2 (MilliporeSigma), anti-H3K27me3 (MilliporeSigma), anti-H4K16ac (MilliporeSigma), and anti–histone H3 (Santa Cruz Biotechnology).

Radioactive assay

HMTase assays were carried out at 30°C overnight in 30-μl volume that contained 20 mM Tris-HCl (pH 8.0), 4 mM EDTA, 1 mM PMSF, 0.5 mM DTT, 100 nCi of *S*-adenosyl-L-methionine (methyl-^{14}C; ^{14}C-SAM; PerkinElmer, Waltham, MA, USA), 15 μg of core histones from calf thymus (MilliporeSigma), and GST-DOT1L, GST-multiple myeloma set domain (MMSET), or GST-SET and MYND domain-containing protein 3 (SMYD3). ^{14}C-labeled histones were subjected to histone demethylase assay using either purified GST or GST-KDM2B$_{1–734}$. Histones were transferred onto p81 filter paper (Upstate) and washed 3 times with 95% ethanol for 5 min at room temperature. Filters were allowed to air dry, and 2 ml of Ultima Gold (PerkinElmer) was then added. ^{14}C-SAM was quantified using a scintillation counter.

Immunofluorescence analysis

293T cells were transfected with the p3XFLAG-CMV-KDM2B wild-type or catalytic mutant using Lipofectamine 2000 Reagent (Thermo Fisher Scientific). Cells were fixed 48 h after transfection, permeabilized, and stained with the appropriate Abs and secondary fluorochrome-labeled Abs. Stained cells were analyzed by confocal laser fluorescence microscopy. The following Abs were used: anti-FLAG, anti-H3K79me3 (Epigentek, Farmingdale, NY, USA), anti-H3K79me1, goat anti-mouse IgG (H+L) FITC conjugated (Bethyl Laboratories, Montgomery, TX, USA), and Cy3-conjugated AffiniPure goat anti-rabbit IgG (H+L) (Jackson ImmunoResearch Laboratories, West Grove, PA, USA).

Histone acid extraction and nucleosome extraction

To extract histones, cell pellets were resuspended in PBS with 0.5% Triton X-100 and protease inhibitors, and tubes were

subsequently incubated at 4°C for 30 min to lyse cells. Lysates were centrifuged at 4°C for 10 min at 10,000 *g*, and pellets were resuspended in 0.4 N H_2SO_4. Samples were centrifuged at 4°C for 10 min at 16,000 *g*. Pellets were again resuspended in 100% trichloroacetic acid and centrifuged at 4°C for 10 min at 16,000 *g*. Histone-containing pellets were collected and eluted in distilled water. To extract nucleosomes, cell pellets were resuspended in RSB buffer (10 mM Tris-HCl, pH 7.4, 10 mM NaCl, 3 mM $MgCl_2$, 0.5% NP-40, 1 mM DTT, and 1 mM PMSF), and tubes were subsequently incubated at 4°C for 30 min to lyse cells. Lysates were centrifuged at 4°C for 5 min at 4000 rpm, and pellets were resuspended in RSB buffer. Samples were sonicated and centrifuged at 4°C for 5 min at 4000 rpm. Pellets were washed 4 times with RSB buffer and eluted in the same buffer.

Luciferase assay

Luciferase assays were conducted using the *HOXA7*, *MEIS1*, simian virus 40, and thymidine kinase promoter reporter systems. 293T cells were cotransfected with the corresponding promoter reporter constructs and the indicated DNA constructs using polyethyleneimine. Cells were harvested after 48 h and assayed for luciferase activity using a luciferase assay system (Promega). Each value is expressed as the mean of 5 replicates of a single assay. All experiments were performed at least 3 times.

Chromatin IP quantitative PCR and chromatin IP sequencing analyses

Formaldehyde (1%) was added to the medium for 10 min at room temperature, followed by addition of 125 mM glycine for 5 min at room temperature. Adherent cells were scraped from dishes into 1 ml PBS. Scraped cells were centrifuged and the resulting pellets were washed once with PBS. Pellets were resuspended in SDS lysis buffer (1% SDS, 10 mM EDTA, and 50 mM Tris-HCl, pH 8.1). Cell lysates were sonicated, diluted with 5 volumes of dilution buffer (0.01% SDS, 1.2 mM EDTA, 1.1% Triton X-100, 167 mM NaCl, and 16.7 mM Tris-HCl, pH 8.1), and incubated overnight with indicated Abs [1 μg Ab for each immunoprecipitation (IP) reaction]. The next day, protein A/G-agarose beads (GenDepot, Barker, TX, USA) were added to the reaction, incubated for 2 h, and washed with low-salt wash buffer, high-salt wash buffer, LiCl immune-wash buffer, and Tris-EDTA buffer. Immunoprecipitates were eluted and reverse crosslinked at 65°C. After, DNA fragments were purified either for PCR amplification or for sequencing using Illumina HiSeq 2000. To analyze promoter regions of *HOXA7*, *MEIS1*, *ALX1*, *GATA4*, and 5′ ends of *PDE3B*, primer sets that consisted of the 123-bp region (27157423–27157545 in chromosome 7), 253-bp region (66434839–66435091 in chromosome 2), 158-bp region (85280099–85280256 in chromosome 12), 172-bp region (11707845–11708016 in chromosome 8), and 165-bp region (14644874–14645038 in chromosome 11) were used.

Values represent means ± SD of technical duplicates from a representative experiment. All experiments were performed 3 times with similar results.

Quantitative PCR analyses

Disassociation curves were generated after each PCR run to ensure the amplification of a single product of the appropriate length. The mean threshold cycle (C_t) and SE values were calculated from individual C_t values obtained from duplicate reactions per stage. Normalized mean C_t value was estimated as ΔC_t by subtracting the mean C_t of the input. The primer concentration used for quantitative PCR (qPCR) (Bio-Rad, Hercules, CA, USA) was 0.2 μM/10 μl. Thermal cycler conditions were as follows: 15 min of holding at 95°C, followed by 39 cycles at 94°C for 15 s, 56°C for 30 s, and 72°C for 30 s.

Statistics

Data were analyzed by Student's *t* tests as indicated.

RESULTS

Identification of the H3K79me2 peptide-interacting proteins

In an attempt to identify a potential H3K79 demethylase, we hypothesized an interaction between H3K79me site and a corresponding demethylase or a certain complex with H3K79 demethylase activity. This hypothesis led us to perform a peptide pull-down assay using H3K79me2 peptides with K562 nuclear extracts. Using LC-MS/MS, we demonstrated that methylated H3K79 was associated with chromobox homolog 8 (CBX8), one of the various types of CBX proteins that direct the canonical PRC1 complex as an interacting component (**Fig. 1*A*, *B*** and Supplemental Table 1). To rule out the possibility of nonspecific binding, we carried out pull-down assays between CBX8 and H3K79me0 peptides as negative controls, and confirmed that CBX8 interacted with H3K79me2 peptides, but not with H3K79me0 peptides (Fig. 1*C*). In addition, we assessed RNF133 and NELFE identified in LC-MS/MS as other candidate proteins and observed that both proteins interacted with H3K79me2 peptides (Supplemental Fig. 1). PRC1, one of the polycomb group (PcG) multiprotein complexes, has a diverse composition that depends on the presence or absence of CBX proteins (46, 47). Previous studies isolated nuclear proteins that were bound to KDM2B and identified the BCL6 corepressor (BCOR) complex by mass spectrometry (48). Other studies identified the presence of the KDM2B-containing noncanonical PRC1-BCOR-CBX8 complex (48, 49). To investigate the associations of these proteins, we performed IP experiments and demonstrated that KDM2B bound CBX8 (Fig. 1*D*). On the basis of these results, we suggest that CBX8 is associated with KDM2B in a certain complex and that KDM2B possibly functions at the H3K79me site.

KDM2B demethylates H3 di-/trimethyl-K79 *in vitro* and *in vivo*

In addition to being a subunit of the noncanonical PRC1 complex, KDM2B is the only known demethylase involved in other types of complexes that contain CBX8, including the BCOR complexes; therefore, we decided to assess the H3K79 demethylation activity of KDM2B (Supplemental Fig. 2*A*). Ectopic expression of FLAG-tagged full-length KDM2B in 293T cells markedly reduced the levels of H3K79me3 and H3K79me2. No decrease in H3K79me1 levels was observed (**Fig. 2*A***, left). As expected, KDM2B also decreased the levels of H3K36me2; however, a mutant form with a substitution of histidine with alanine in the JmjC domain

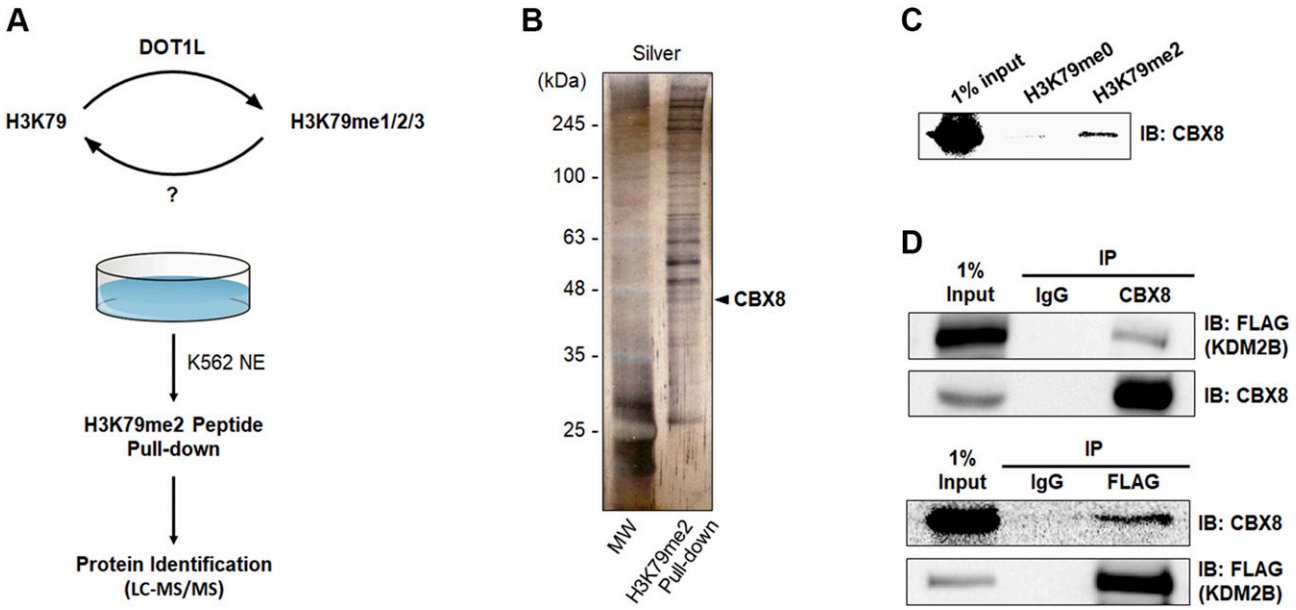

Figure 1. Identification of H3K79me2-associated proteins. *A*) Schematic representation of pull-down assay using H3K79me2 peptides in K562 nuclear extract. *B*) The pull-down complex was separated by using 12% SDS-PAGE and visualized with silver staining. Gel was sliced into 3 sections and subjected to LC-MS/MS analysis. Several peptide sequences that contained CBX8 fragments were detected. *C*) Pull-down of H3K79me2 and H3K79me0 (as a negative control) in K562 whole-cell lysate. *D*) IP of endogenous CBX8 and ectopically overexpressed FLAG-KDM2B in 293T cells.

that is catalytically deficient in H3K36 demethylase activity, KDM2B-H242A, failed to demethylate H3K79me3, H3K79me2, and H3K79me1 (Fig. 2*A*, left). We also found no change in H3K9 and H3K27 methyl marks by KDM2B (Supplemental Fig. 2*B*). In addition, we observed that DOT1L rescued the effects of KDM2B on H3K79, but not on H3K36, which indicates the H3K79 specificity of KDM2B (Supplemental Fig. 2*C*).

We next investigated the H3K79 demethylation at the global level by comparing methylation status in stable KDM2B knockdown 293T cells. We used 2 independent shRNAs that target different regions of KDM2B: one in the CDS and the other in the 3′-UTR. We found that RNA interference of endogenous KDM2B led to increased H3K79me3 and H3K79me2 levels, but monomethylation was not affected (Fig. 2*A*, right). Furthermore, immunocytochemistry demonstrated that overexpression of KDM2B in 293T cells resulted in a loss of H3K79me3, which was in contrast with the strong H3K79me3 staining signals observed in adjacent nontransfected cells (Fig. 2*B*); however, overexpression of KDM2B had no detectable effect on H3K79me1 levels determined by immunocytochemistry (Fig. 2*B*).

We confirmed the H3K79 demethylase activity of KDM2B through *in vitro* assays. It was necessary to decide whether the above observations derived from indirect effects of genetic manipulation or from direct enzymatic activity of KDM2B. After incubation of core histones with increasing concentrations of GST-KDM2B that contained the JmjC, CXXC, and plant homeodomain domains (1–734 aa), we observed reduced levels of H3K79me2 and H3K79me3 (Fig. 2*C*, left). We examined the effects of KDM2B on nucleosomes. Similar to the effects on core histones, KDM2B demethylated both H3K79me2 and H3K79me3 of nucleosomes (Fig. 2*C*, right). Consistent with results from *in vivo* analysis of H3K79 methylation patterns, *in vitro* assay using nucleosomes, including catalytically inactive recombinant KDM2B-H242A, did not alter H3K79me3 level (Supplemental Fig. 2*D*). We concluded that KDM2B had H3K79 demethylase activity both *in vitro* and *in vivo*. We performed isothermal titration calorimetry experiments to assess the binding affinity of KDM2B toward trimethylated H3K79 peptides. Given that H3K79me3 had a lower dissociation constant than H3K79me0, GST-KDM2B$_{1–734}$ bound to H3K79me3 with stronger affinity (Supplemental Fig. 3*A*). To demonstrate the specificity toward H3K79, we assessed whether KDM2B removes methyl groups from recombinant histone H3 with MLAs, which was specifically methylated by chemical alkylation reaction (43, 44), using FDH assays. FDH assay measures the production of formaldehyde, a byproduct derived from demethylation reaction, by monitoring the reduction of NAD^+ into NADH (45, 50). We used a fluorescence-based detection method and assessed the demethylase activity of KDM2B. It was observed that KDM2B effectively produced marked amounts of formaldehyde from MLA histone H3 that contained trimethylation on K_c79, which confirmed that H3K79 is a substrate for demethylation catalyzed by KDM2B (Fig. 2*D*). The FDH assay system also worked for MLA histone H3K$_c$36me2 as a substrate (Supplemental Fig. 3*B*). Furthermore, we performed *in vitro* histone demethylase assays and LC-MS/MS analysis with MLA histone H3K$_c$79me3. Incubation with GST-KDM2B$_{1–734}$ led to demethylation of MLA histone H3K$_c$79me3 and an increase of H3K$_c$79me1 level (Supplemental Fig. 3*C*). Western blot analysis of MLA histone H3K$_c$79me3 incubated with GST-KDM2B$_{1–734}$ confirmed a marked

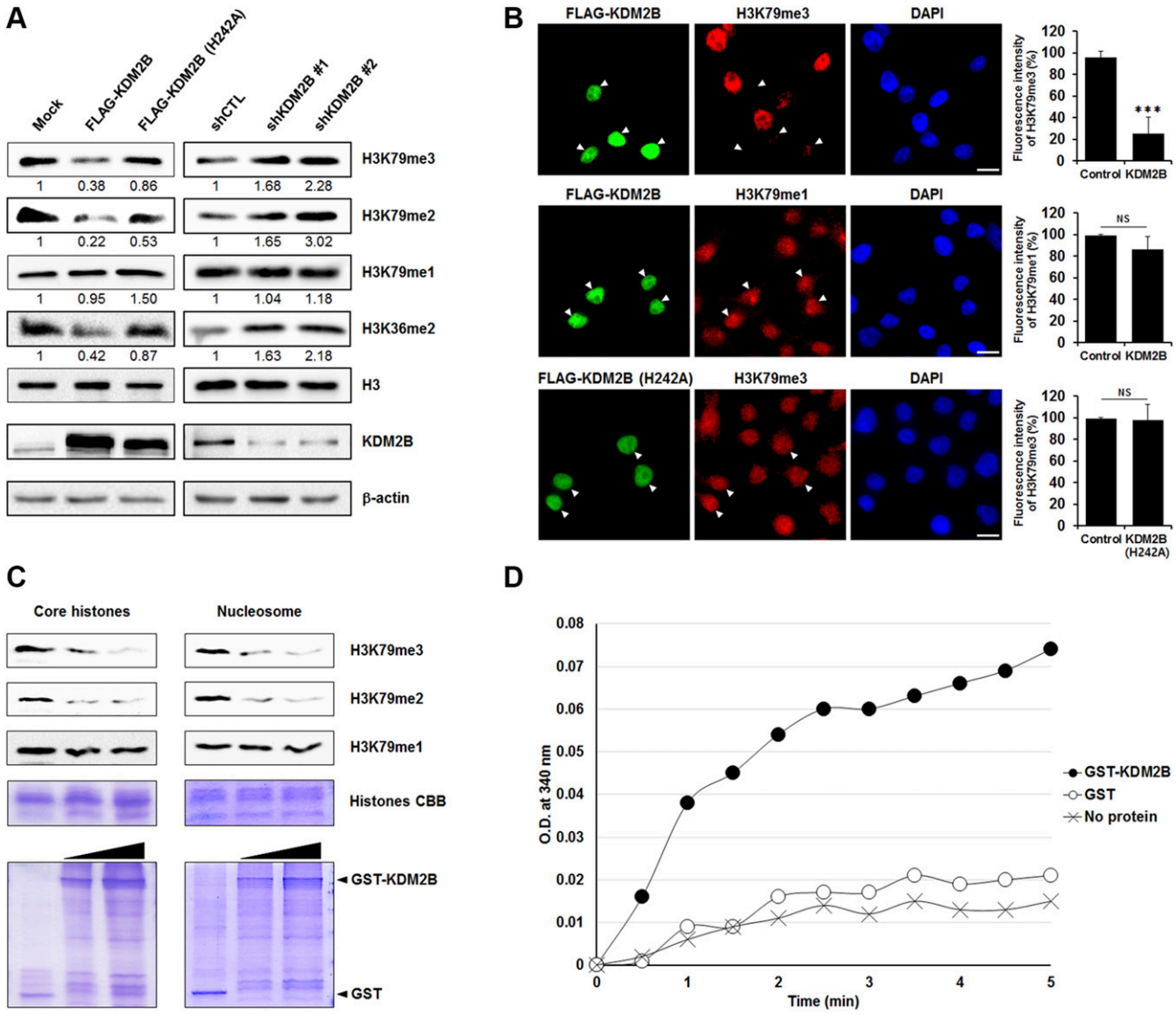

Figure 2. KDM2B demethylates histone H3K79me2/3. *A*) Effects of overexpression and knockdown of KDM2B on H3K79 demethylation. FLAG-tagged KDM2B wild-type and catalytically deficient H242A mutant were transfected into 293T cells. H3K79me1/2/3 levels were detected with Western blot analysis. KDM2B knockdown stable 293T cells were analyzed in the same way. *B*) Immunocytochemistry of 293T cells that expressed FLAG-KDM2B wild-type and KDM2B-H242A. Changes in signal intensity were detected after double immunostaining with anti-FLAG and anti-H3K79me1/3 Abs. Arrows indicate transfected cells. Scale bars, 10 μm. *C*) KDM2B *in vitro* demethylase assay. Core histones and nucleosomes were used as substrates (top). Demethylation activity of KDM2B against di- and trimethyl H3K79 is shown. Purified GST and GST-KDM2B$_{1–734}$ recombinant proteins used were visualized by Coomassie staining (bottom). *D*) Formaldehyde production was detected by FDH assay. NADH production was measured at OD 340 nm after a 3-h reaction using GST-KDM2B, together with recombinant MLA histone H3K79me3 as substrates. Absence of demethylase and GST were used as negative controls.

decrease in H3K79me3 level (data not shown). Results indicate that KDM2B is an H3K79me2/3-specific demethylase.

Structural analysis of H3K79 demethylation by KDM2B

To obtain insights into the mechanism of the demethylation reaction, we modeled H3K79 onto the KDM2B structure on the basis of the H3K36-bound KDM2A structure determined by Cheng *et al.* (51). Given that the location of H3K79 within the protein structure is in the loop between the 2 α-helices, this region could be accessible to the active site of KDM2B with a slight conformational change. Remarkably, the sequences around the K79 and K36 of histone H3 are similar in their chemical properties. In accordance with the sequence alignment of residues that surround H3K79 and H3K36 (**Fig. 3*A***), this modeling exercise indicated that the hydrophobic residues in the H3K79 peptide—Phe78, Leu82, and Phe84—are involved in hydrophobic interactions with KDM2B (Fig. 3*B*). This is similar to what occurs in the interactions of the H3K36 peptide with the complex structure of KDM2A. The residues—His242 and His314—for binding of iron and α-ketoglutarate were also conserved in the modeled structure (Fig. 3*B*), which indicates concomitant bindings

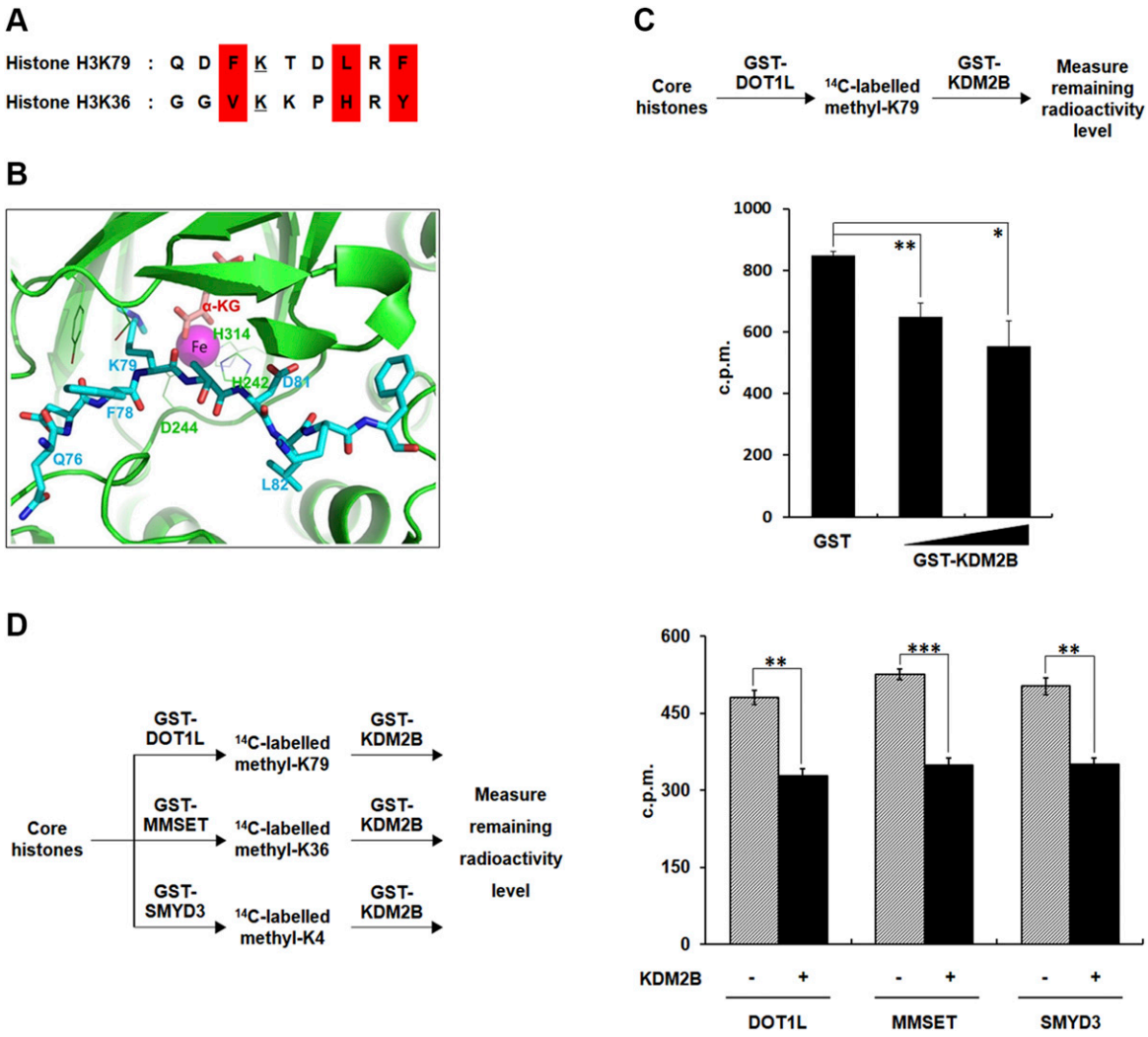

Figure 3. Structural modeling of KDM2B demethylase activity. *A*) Comparative sequence analysis of 9 aa around K36 and K79 of histone H3. *B*) Crystal structure of KDM2B with enlarged residues critical for binding to H3K79. Iron cofactor and H3K79 residues in the catalytic pocket are shown. *C*) Radioactive assay using core histones. H3K79 residues were ^{14}C-labeled by GST-DOT1L *via* histone methyltransferase assay, and histones were used in histone demethylase assays with GST-KDM2B. Remaining radioactivity levels from histones were measured using scintillation counting to assess demethylase activity. All error bars indicate SEM for at least triplicate experiments. *D*) Radioactive assays using core histones. H3K79, H3K36, and H3K4 residues were ^{14}C labeled by DOT1L, MMSET, and SMYD3, respectively. ^{14}C-labeled histones were used in histone demethylase assays with KDM2B. Remaining radioactivity levels from histones were measured using scintillation counting to assess demethylase activity. All error bars indicate SEM for at least triplicate experiments.

of these cofactors with the H3K79 peptide. Together, these findings indicate that H3K79 is a plausible demethylation site for KDM2B.

We also verified the H3K79 demethylase activity of KDM2B using core histone substrates that were radiolabeled by DOT1L, which is responsible for methylation at K79 sites. KDM2B significantly decreased the levels of H3K79-methylated histones (Fig. 3*C*). In addition, as KDM2B was well known as H3K36 and H3K4 demethylase (31–33), we compared the activities of KDM2B between H3K79, H3K36, and H3K4 using ^{14}C-labeled histones by DOT1L, MMSET, and SMYD3, respectively (Supplemental Fig. 4). We detected considerable reductions in the radioactivity of each histone substrate after demethylation by KDM2B (Fig. 3*D*); therefore, these findings suggest that H3K79 demethylase activity of KDM2B is catalytically effective on the basis of the degrees of H3K36 and H3K4 demethylation.

KDM2B induces transcriptional repression

As H3K79me was involved in transcriptional activation (17–21), we speculated that demethylation of the site by KDM2B might induce transcriptional repression. To elucidate the effects of KDM2B on target gene expression, we first assessed whether KDM2B specifically down-regulated transcription of the 2 best-studied mixed lineage leukemia (MLL) fusion target loci, the *HOXA7* and *MEIS1*, that are preferentially regulated by changes in H3K79me level. Luciferase reporter assays demonstrated that KDM2B overexpression resulted in *HOXA7* and *MEIS1* transcriptional down-regulation, and, conversely,

that KDM2B knockdown resulted in their up-regulation (**Fig. 4*A***). These results are consistent with the previously examined repressive function of KDM2B. To show whether the enzymatic activity of KDM2B was required for the repressive function of the protein, the catalytically inactive mutant (H242A) and ΔCXXC mutant were tested in reporter assays using the *HOXA7* promoter. A significant absence of transcriptional repression was observed in assays using the ΔCXXC mutant, and partial repression was observed in assays using the H242A point mutant (Fig. 4*B*). To examine whether demethylation of H3K79 catalyzed by KDM2B led to down-regulation of general transcription, we carried out luciferase assays using simian virus 40 and thymidine kinase promoters. Transient overexpression of KDM2B repressed luciferase activity on both promoters, whereas KDM2B depletion resulted in transcriptional activation (Supplemental Fig. 5). We next investigated whether transcriptional activities of KDM2B and DOT1L were in opposite directions *via* regulation of H3K79me. Knockdown of DOT1L recapitulated KDM2B-mediated transcriptional repression on the same 2 promoters (data not shown).

On the basis of published data, we selected 4 genes from ~2500 genes that are directly targeted by KDM2B. *HOXA7*, *MEIS1*, *ALX1*, and *GATA4* have been reported as KDM2B and PcG target genes by chromatin IP (ChIP) sequencing (seq) and ChIP analyses using mouse embryonic stem cells (34–36, 52). Using these 4 known target genes, we demonstrated that H3K79 demethylation alone, without H3K36 or H3K4 demethylation, was involved in KDM2B-mediated repression. We measured the transcription levels of the 4 target genes using wild-type and K4/36R mutant histone H3. As expected, these 4 genes demonstrated clear down-regulation in H3 K4/36R-overexpressing stable cells, similar to their levels in H3 wild-type–overexpressing stable cells when KDM2B was ectopically expressed (Fig. 4*C*). Taken together, we established that H3K79 demethylation is indeed required for KDM2B-mediated repression in addition to H3K36 and H3K4 demethylations.

KDM2B depletion regulates gene expression through genome-wide accumulation of H3K79me

To determine the global location of H3K79me sites under the influence of KDM2B, we performed ChIP-seq in KDM2B knockdown stable 293T cells. A comparison of the 2 ChIP-seq data sets—control shRNA *vs.* shKDM2B—using heat maps demonstrated that, at the global human genome level, H3K79me3 was enriched under the condition of KDM2B depletion (**Fig. 5*A***). Normalized sequencing depth of ChIP-seq data revealed that, under the KDM2B knockdown condition, methylation marks were considerably enriched around the centers of H3K79me3 peaks, which suggests that KDM2B ablation strongly up-regulated H3K79me3 (Fig. 5*B*). We confirmed that marked

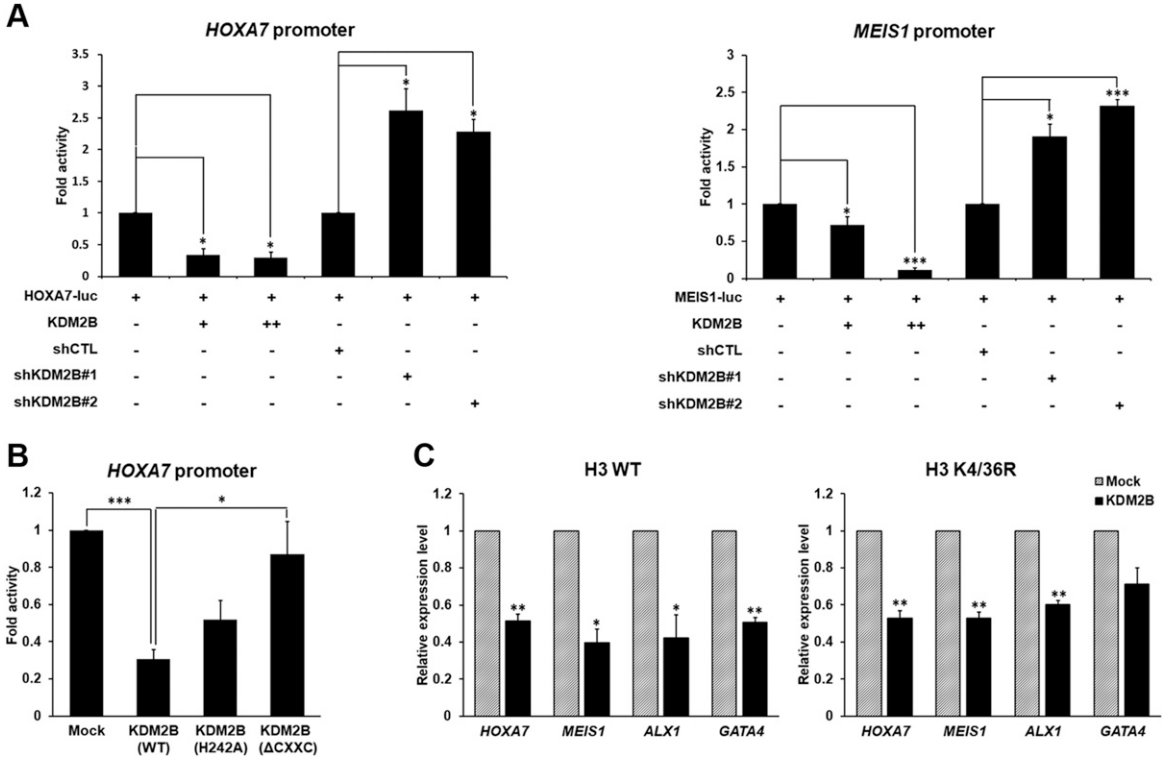

Figure 4. KDM2B-mediated transcriptional repression *via* H3K79 demethylation. *A*) Luciferase assay using KDM2B target gene promoters. Promoter activities were analyzed with overexpression or depletion of KDM2B. All values are shown as SEM, $n = 3$. *B*) Luciferase assays using catalytically inactive mutants and deletion mutants of KDM2B. All values are shown as SEM. *C*) RT-qPCR analysis of target gene expression in cells that stably overexpressed histone H3 wild-type or K4/36R mutant. All error bars indicate SEM for at least triplicate experiments. $^{*}P < 0.05$, $^{**}P < 0.01$, $^{***}P < 0.001$.

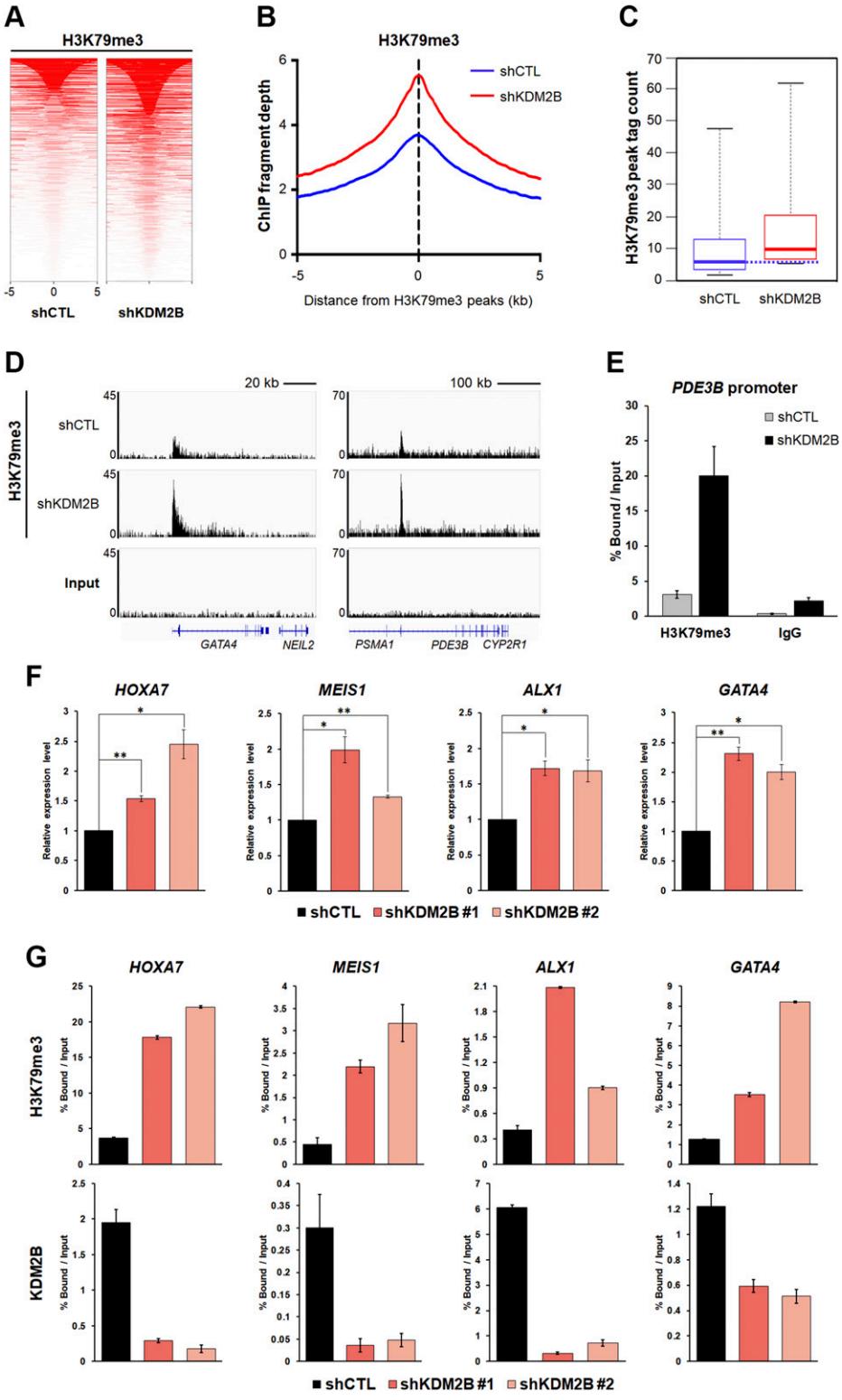

Figure 5. KDM2B lowers H3K79me3 occupancy at target gene promoters. *A*) ChIP-seq heat map covering 10-kb regions across H3K79me3 peaks. *B*) H3K79me3 ChIP-seq signal normalized by input sample in control (blue line) and shKDM2B cells (red line). *C*) Change in H3K79me3 occupancy after KDM2B knockdown. *D*) Input and H3K79me3 ChIP-seq profiles over 2 regions of the genome in control and shKDM2B cells. Below the sequencing traces, *GATA4* and *PDE3B* genes are indicated. *E*) H3K79me3 mark at *PDE3B* promoter in KDM2B knockdown cells analyzed by ChIP-qPCR. *F*) RT-qPCR analysis for the detection of target gene expression. KDM2B was depleted in 293T cells. *G*) ChIP-qPCR analysis for the measurement of KDM2B enrichment and H3K79me3 levels on target gene promoters. KDM2B was stably knocked down in 293T cells. Promoters of *HOXA7*, *MEIS1*, *ALX1*, and *GATA4* were immunoprecipitated and amplified using specific primers. Values represent means ± SD of technical duplicates from a representative experiment. All experiments were performed 3 times with similar results.

increases in H3K79me3 occupancy—at the genome-wide level—were correlated with KDM2B knockdown by analyzing mean ChIP-seq tag density of shKDM2B compared with that of control shRNA (Fig. 5*C*). ChIP-seq binding profiles on individual genes, such as *GATA4* and *PDE3B*, clearly indicated that H3K79me3 levels were up-regulated in the shKDM2B stable cell line (Fig. 5*D*). To validate the ChIP-seq experiment, we selected a KDM2B-responsive gene, *PDE3B*, and performed ChIP qPCR. H3K79me3 accumulated on the *PDE3B* promoter when KDM2B was depleted (Fig. 5*E*). To characterize chromatin profiles near transcription start sites of H3K79me3-occupied genes that are sensitive to KDM2B depletion, we compared H3K79me3 peaks with published ChIP-seq studies for KDM2B in human acute myeloid leukemia cells (53). We noticed that alterations of H3K79me were correlated with

KDM2B binding. KDM2B peaks were localized at *EGLN1* and *CYFIP1* loci, and H3K79me3 occupancy increased at these 2 genes after KDM2B depletion (Supplemental Fig. 6*A*). Sixty-one percent of genes that had >2-fold change in H3K79me3 levels overlapped with KDM2B target genes (Supplemental Fig. 6*B*). Genes whose H3K79me3 levels increased under the shKDM2B condition were selected and categorized by gene ontology term analysis (Supplemental Fig. 6*C*). Of note, these genes were related to well-known functions of H3K79me, including transcriptional regulation and cell-cycle control. Results suggest that KDM2B is responsible for a considerable amount of H3K79 demethylation that occurs on its target genes.

We next sought to understand the effects of KDM2B recruitment on the levels of H3K79me3 on target gene promoters. We performed ChIP-qPCR analyses. Overexpression of wild-type KDM2B considerably decreased H3K79me3 levels on the promoters of 4 genes tested and led to transcriptional repression (Supplemental Fig. 7*A*, *B*). In contrast, the catalytically deficient KDM2B mutant failed to change H3K79me levels and gene expression, although it was still recruited to target promoters (Supplemental Fig. 7*A*, *B*). Using 2 independent KDM2B knockdown stable cell lines, we observed clear increases in H3K79me3 deposition on the *HOXA7*, *MEIS1*, *ALX1*, and *GATA4* promoters and concomitant induction of these target genes expression (Fig. 5*F, G*). We obtained similar results when ChIP experiments were normalized to histone H3 occupancy (Supplemental Fig. 7*C*). In addition, normalized ChIP results for H3K36me2 and H3K4me3 as well as H3K79me3 support the working model of KDM2B-mediated demethylation in a way of targeting multiple sites (Supplemental Fig. 7*D*). Collectively, these data demonstrate that KDM2B is recruited to specific target gene promoters and demethylates H3K79me3, which results in the down-regulation of transcription.

Recruitment of SIRT1 protein to target gene promoters by KDM2B

Previous studies have demonstrated that H3K79me by Dot1 regulated gene silencing (10, 11, 54). Silent information regulator proteins preferentially bind chromatin that contains hypomethylated H3K79 and block H3K79me (17). As a member of the sirtuin family of proteins, SIRT1 is the human homolog of the yeast Sir2 protein and mediates deacetylation of histones H3, H4, and H1 (55). To delineate the relationship between H3K79 demethylation and silent information regulator protein-mediated transcriptional repression, we assessed whether KDM2B induced recruitment of SIRT1 to the target gene promoters. We measured levels of SIRT1 and H4K16ac on the *HOXA7*, *MEIS1*, *ALX1*, and *GATA4* promoters by ChIP qPCR analysis in KDM2B knockdown stable cell lines. We found that depletion of KDM2B increased H3K79me3 levels (Fig. 5*G*), which led to the disruption of chromatin binding of SIRT1 and an increase in H4K16ac levels (**Fig. 6*A***). Enrichment of H4K16ac under KDM2B ablation provides evidence for a correlation between H3K79me and H4K16ac in transcriptional up-regulation. A recent study on the functional interplay between DOT1L and bromodomain-containing protein 4 reported that H3K79me, by itself, was not necessary for transcriptional activation, and that H4 acetylation was required for the actual regulatory effects to occur as downstream events (56). To evaluate a model of SIRT1 recruitment, we overexpressed KDM2B in the KDM2B knockdown stable cell line. As expected, H3K79 hypomethylation-facilitated SIRT1 binding was rescued by ectopic KDM2B (Supplemental Fig. 8*A*). We tested whether KDM2B interacted with SIRT1. IP analysis in 293T cells that overexpressed KDM2B and SIRT1 demonstrated that KDM2B bound SIRT1, and the interaction between endogenous SIRT1 and KDM2B was also detected (Fig. 6*B, C*). SIRT1 has been demonstrated to inhibit chromatin binding of DOT1L by H3K9me2 accumulation and chromatin compaction *via* SUV39H1 localization (57). To examine whether the decreases in H3K79me levels mediated by KDM2B were a result of its association with SIRT1 and concomitant failure of DOT1L recruitment, we performed IP assay in wild-type and catalytic mutant of KDM2B overexpressed cells and confirmed that KDM2B-H242A also bound SIRT1 (Supplemental Fig. 8*B*). Given that KDM2B-H242A did not alter H3K79me3 levels, as shown in Fig. 2*A* and Supplemental Fig. 7*B*, we concluded that H3K79me reduction by KDM2B did not originate from DOT1L inaccessibility caused by KDM2B-SIRT1 interaction. This interaction suggests that KDM2B induces SIRT1 recruitment, possibly *via* H3K79 demethylation, and facilitates H4K16 deacetylation. To demonstrate the role of SIRT1 recruitment in transcriptional repression by KDM2B, we assessed whether the SIRT1 inhibitor (sirtinol) abolished KDM2B-mediated repression. Treatment with sirtinol resulted in a marked recovery of transcription of KDM2B target genes despite KDM2B overexpression (Fig. 6*D*). This is consistent with results of a previous study that described the requirement for H4 acetylation in transcriptional activity *via* alteration of H3K79me levels (56). Taken together, these results indicate that H3K79 demethylation by KDM2B and the subsequent tethering of SIRT1 are both involved in KDM2B-mediated transcriptional repression.

DISCUSSION

Although H3K79 is located in the globular domain of histone H3, it is localized on the surface of the nucleosomal structure and can be accessed by epigenetic modifiers (10). That H3K79me is evolutionarily conserved in a variety of eukaryotes is a strong indication of its fundamental role in the regulation of chromatin structure (58). Although extensive studies have been conducted to characterize the role of H3K79me in transcriptional regulation and its physiologic outcome, the identity of the H3K79 demethylase has been uncertain. In the current study, we have identified KDM2B as a histone H3K79me2/3 demethylase. Using a pull-down assay followed by mass spectrometry analyses, we identified H3K79me2-interacting proteins, including CBX8. As a component of the canonical PRC1 complex, CBX8 recognizes the H3K27me3 site and

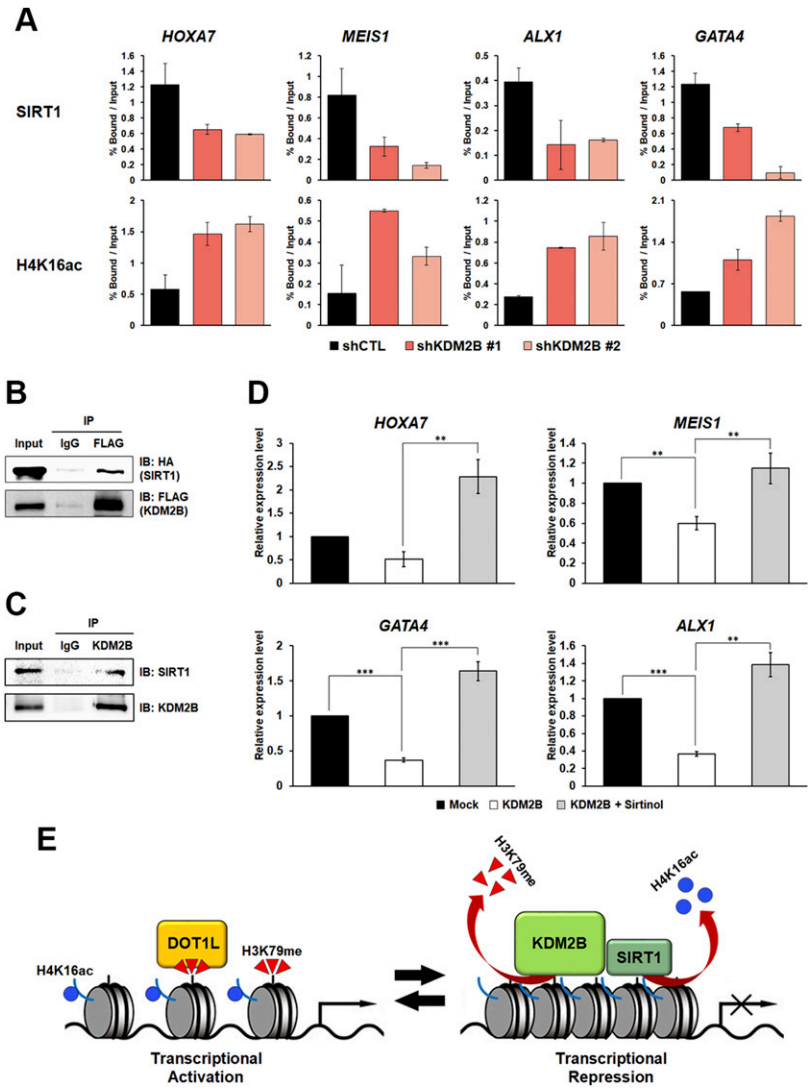

Figure 6. KDM2B-mediated H3K79 demethylation induces recruitment of SIRT1 to chromatin. *A*) ChIP analysis was performed using anti-SIRT1 and anti-H4K16ac Abs in stable KDM2B knockdown 293T cells. Immunoprecipitated DNA fragments were analyzed by RT-qPCR from the promoter regions of *HOXA7*, *MEIS1*, *ALX1*, and *GATA4*. Values represent means ± SD of technical duplicates from a representative experiment. All experiments were performed 3 times with similar results. *B*) IP of ectopically overexpressed FLAG-KDM2B in 293T cells that were transfected with FLAG-KDM2B and hemagglutinin-SIRT1. *C*) IP of endogenous KDM2B in 293T cells. *D*) RT-qPCR analysis for the detection of target gene expression. 293T cells were treated with DMSO or sirtinol for 2 h after KDM2B overexpression. All error bars indicate SEM for at least triplicate experiments. *E*) Proposed model of transcriptional repression of target genes by KDM2B *via* H3K79 demethylation and SIRT1 recruitment.

interacts with RING1B to contribute to H2AK119ub1 and the maintenance of the transcriptionally repressive state (46, 47). The noncanonical PRC1-BCOR-CBX8 complex represses bivalent promoters and contains KDM2B as a component (49). In contrast, CBX8 interacts with MLL-AF9 and TIP60, playing a role in transcriptional activation of MLL-AF9 target genes (59). It is possible that CBX8 regulates gene expression in both positive and negative ways, depending on the enzymatic properties of binding partners, by serving as a molecular adaptor that localizes catalytic subunits in the complex to target genes. The reason why H3K79me2 and CBX8 protein interact requires additional investigation.

KDM2B is a member of the F-box protein family that includes KDM2A and which also shows H3K36 demethylase activity. KDM2B and KDM2A share conserved domains, including the JmjC and CXXC domains, and both proteins bind CpG islands (60). They both catalyze the demethylation of H3K36me2, which is a highly abundant modification and is specifically depleted at CpG islands (60). According to studies of different H3K27 demethylase activities of UTX and UTY (61, 62), it remains to be investigated whether KDM2A also catalyzes H3K79 demethylation. KDM2A does not associate with PcG proteins, and its function in transcriptional regulation differs subtly from that of KDM2B.

H3K79me is found throughout the euchromatic regions of the genomes of yeast and higher eukaryotes, but is significantly under-represented in silent chromatin (17). Sir2, which is involved in heterochromatin formation, is not recruited to the region of the chromosome that contains H3K79me in yeast (54). H3K79me2 is excluded from telomeres and mating-type loci to which Sir2 is recruited and mediates heterochromatin formation (10, 63). H3K79me2/3 is also associated with active gene expression in yeast and mammalian cells (63, 64). A recent study suggested that the inactivation of DOT1L in MLL-AF9 leukemia cells enhanced SIRT1 occupancy at most genes marked with H3K79me, which demonstrates an antagonistic relationship between DOT1L and SIRT1 (57). In fact, the heterochromatin proteins, Sir3 and Dot1, compete for the basic patch of histone H4 in yeast. H4K16ac by Sas2 displaces Sir3 and enables Dot1 to bind H3K79, which methylates H3K79 (65, 66).

The current study reveals that KDM2B is an H3K79me2/3 demethylase and acts as a transcriptional

corepressor. Using ChIP-seq and ChIP qPCR analyses, we determined that KDM2B led to the loss of H3K79me on target genes. Of interest, a previous study found that knockout of DOT1L reduced H3K79me2 globally, but resulted in only a subset of H3K79me2/3 marked loci to be down-regulated (30). In addition, the effects of individual epigenetic modifiers on gene expression were much more specific and limited than were predicted by changes in the status of a single histone modification (67). On the basis of these studies, we concluded that even though KDM2B influenced H3K79me at a genome-wide level, additional gene-dependent and context-dependent mechanisms might be involved in the regulation of gene expression. Recent studies have demonstrated the role of histone H4 acetylation as a link between H3K79me and transcriptional activation (56). This suggests the importance of a particular chromatin context in the regulatory processes that are mediated by changes in H3K79 methylation. We provided evidence that KDM2B induced the recruitment of SIRT1 to target gene promoters, which led to H4K16 deacetylation and chromatin silencing. This is consistent with an earlier report that CBX8 is a binding partner of SIRT1 and that both cooperatively mediate transcriptional repression (68).

To rule out the hypothesis that KDM2B-mediated repression in our study was derived from the demethylation of 2 previously known substrates of KDM2B, H3K4, and H3K36, we overexpressed K4/36R double-mutant histone H3 that was not subjected to methylation or demethylation. Transient overexpression of KDM2B after the selection of H3 K4/36R-overexpressing stable cells enabled us to rule out the repressive effects of K4 and K36 demethylation as an explanation and enabled us to propose an independent mechanism with a new target residue, K79. The wide histone substrate repertoire for KDM2B demethylase activity, which includes H3K36, H3K4, and H3K79, is interesting and suggests the possibility that KDM2B may also have nonhistone protein substrates. In addition, considering the identification of new H3K79 HMTases other than DOT1L, it is reasonable to speculate that there may be other H3K79 demethylases in addition to KDM2B yet to be identified.

Given that the H3K36 demethylase activity of KDM2B was not necessary for its variant PRC1-mediated H2AK119ub1 and transcriptional repression, we determined whether H2AK119ub1 was required to enable the H3K79 demethylase activity of KDM2B in the variant PRC1 complex. To test this, we used PRT4165, a potent inhibitor of PRC1-mediated histone H2A ubiquitylation. H2AK119ub1 levels decreased in the presence of PRT4165, but H3K79me3 demethylation catalyzed by KDM2B was not altered, which suggests that the H3K79 demethylase activity of KDM2B was independent of PRC1-mediated H2AK119ub1 (data not shown); however, *via* demethylation of H3K79, KDM2B could possibly play a role in ensuring that genes that are associated with H2AK119ub1 by PRC1 are also trimethylated on H3K27 by PRC2 (69).

In summary, we provide *in vitro* and *in vivo* evidence for the possible role of KDM2B as an H3K79me2/3 demethylase and a corepressor that regulates gene transcription *via* SIRT1-mediated chromatin silencing. Our model suggests that dynamic reversible regulation of histone methylation is indeed applied to H3K79 methylation. This model supports the existence of H3K79 demethylation by KDM2B and its role in transcriptional regulation (Fig. 6*E*). FJ

ACKNOWLEDGMENTS

The authors thank Dr. Jin Young Kim and Dr. Ju Yeon Lee (Korea Basic Science Institute, Ochang Headquarters, Division of Bioconvergence Analysis) for nano–liquid chromatography LTQ-Orbitrap analysis. ChIP-seq data are available from the Gene Expression Omnibus under Accession No. GSE89052. The authors thank Dr. Vivian Bardwell (University of Minnesota, Minneapolis, MN, USA) for providing EFplink2-FLAG-KDM2B. This work was supported by the Chung-Ang University Excellent Student Scholarship in 2013 (to J.-Y.K.); Grant NRF-2016R1A4A1008035 (to J.-Y.K., J.W.P., H.C., J.Y.H., and Y.-C.C.) from the National Research Foundation of Korea (NRF), funded by the Ministry of Science, Information and Communication Technology (ICT), and Future Planning; and Grant NRF-2017R1A2B4004407 (to J.-Y.K. and J.Y.H.) funded by the Ministry of Science and Technology, Basic Science Research Program. The authors declare no conflicts of interest.

AUTHOR CONTRIBUTIONS

J.-Y. Kang and S.-B. Seo and designed the research and wrote the paper; J.-Y. Kang, K.-B. Kim, J. W. Park, H. Cho, J. Y. Hahm, Y.-C. Chae, and D. Kim performed the research and analyze the data; J.-Y. Kang, J.-Y. Kim, and S.-B. Seo contributed to the analysis and manuscript preparation; H. Kook and S. Rhee helped perform the research; and N.-C. Ha contributed to constructive discussions.

REFERENCES

1. Cheung, P., Allis, C. D., and Sassone-Corsi, P. (2000) Signaling to chromatin through histone modifications. *Cell* **103**, 263–271
2. Strahl, B. D., and Allis, C. D. (2000) The language of covalent histone modifications. *Nature* **403**, 41–45
3. Berger, S. L. (2007) The complex language of chromatin regulation during transcription. *Nature* **447**, 407–412
4. Lee, J. S., Smith, E., and Shilatifard, A. (2010) The language of histone crosstalk. *Cell* **142**, 682–685
5. Wysocka, J., Milne, T. A., and Allis, C. D. (2005) Taking LSD 1 to a new high. *Cell* **122**, 654–658
6. Martin, C., and Zhang, Y. (2005) The diverse functions of histone lysine methylation. *Nat. Rev. Mol. Cell Biol.* **6**, 838–849
7. Mosammaparast, N., and Shi, Y. (2010) Reversal of histone methylation: biochemical and molecular mechanisms of histone demethylases. *Annu. Rev. Biochem.* **79**, 155–179
8. Feng, Q., Wang, H., Ng, H. H., Erdjument-Bromage, H., Tempst, P., Struhl, K., and Zhang, Y. (2002) Methylation of H3-lysine 79 is mediated by a new family of HMTases without a SET domain. *Curr. Biol.* **12**, 1052–1058
9. Lacoste, N., Utley, R. T., Hunter, J. M., Poirier, G. G., and Côte, J. (2002) Disruptor of telomeric silencing-1 is a chromatin-specific histone H3 methyltransferase. *J. Biol. Chem.* **277**, 30421–30424
10. Van Leeuwen, F., Gafken, P. R., and Gottschling, D. E. (2002) Dot1p modulates silencing in yeast by methylation of the nucleosome core. *Cell* **109**, 745–756
11. Singer, M. S., Kahana, A., Wolf, A. J., Meisinger, L. L., Peterson, S. E., Goggin, C., Mahowald, M., and Gottschling, D. E. (1998) Identification of high-copy disruptors of telomeric silencing in *Saccharomyces cerevisiae*. *Genetics* **150**, 613–632

12. Woo Park, J., Kim, K. B., Kim, J. Y., Chae, Y. C., Jeong, O. S., and Seo, S. B. (2015) RE-IIBP methylates H3K79 and induces MEIS1-mediated apoptosis *via* H2BK120 ubiquitination by RNF20. *Sci. Rep.* **5**, 12485
13. Morishita, M., Mevius, D., and di Luccio, E. (2014) *In vitro* histone lysine methylation by NSD1, NSD2/MMSET/WHSC1 and NSD3/WHSC1L. *BMC Struct. Biol.* **14**, 25
14. Luger, K., Mäder, A. W., Richmond, R. K., Sargent, D. F., and Richmond, T. J. (1997) Crystal structure of the nucleosome core particle at 2.8 A resolution. *Nature* **389**, 251–260
15. Ng, H. H., Xu, R. M., Zhang, Y., and Struhl, K. (2002) Ubiquitination of histone H2B by Rad6 is required for efficient Dot1-mediated methylation of histone H3 lysine 79. *J. Biol. Chem.* **277**, 34655–34657
16. Briggs, S. D., Xiao, T., Sun, Z. W., Caldwell, J. A., Shabanowitz, J., Hunt, D. F., Allis, C. D., and Strahl, B. D. (2002) Gene silencing: *trans*-histone regulatory pathway in chromatin. *Nature* **418**, 498
17. Ng, H. H., Ciccone, D. N., Morshead, K. B., Oettinger, M. A., and Struhl, K. (2003) Lysine-79 of histone H3 is hypomethylated at silenced loci in yeast and mammalian cells: a potential mechanism for position-effect variegation. *Proc. Natl. Acad. Sci. USA* **100**, 1820–1825
18. Okada, Y., Feng, Q., Lin, Y., Jiang, Q., Li, Y., Coffield, V. M., Su, L., Xu, G., and Zhang, Y. (2005) hDOT1L links histone methylation to leukemogenesis. *Cell* **121**, 167–178
19. Okada, Y., Jiang, Q., Lemieux, M., Jeannotte, L., Su, L., and Zhang, Y. (2006) Leukaemic transformation by CALM-AF10 involves upregulation of Hoxa5 by hDOT1L. *Nat. Cell Biol.* **8**, 1017–1024
20. Schübeler, D., MacAlpine, D. M., Scalzo, D., Wirbelauer, C., Kooperberg, C., van Leeuwen, F., Gottschling, D. E., O'Neill, L. P., Turner, B. M., Delrow, J., Bell, S. P., and Groudine, M. (2004) The histone modification pattern of active genes revealed through genome-wide chromatin analysis of a higher eukaryote. *Genes Dev.* **18**, 1263–1271
21. Vakoc, C. R., Sachdeva, M. M., Wang, H., and Blobel, G. A. (2006) Profile of histone lysine methylation across transcribed mammalian chromatin. *Mol. Cell. Biol.* **26**, 9185–9195
22. Nguyen, A. T., and Zhang, Y. (2011) The diverse functions of Dot1 and H3K79 methylation. *Genes Dev.* **25**, 1345–1358
23. Wysocki, R., Javaheri, A., Allard, S., Sha, F., Côté, J., and Kron, S. J. (2005) Role of Dot1-dependent histone H3 methylation in G1 and S phase DNA damage checkpoint functions of Rad9. *Mol. Cell. Biol.* **25**, 8430–8443
24. Huyen, Y., Zgheib, O., Ditullio, R. A., Jr., Gorgoulis, V. G., Zacharatos, P., Petty, T. J., Sheston, E. A., Mellert, H. S., Stavridi, E. S., and Halazonetis, T. D. (2004) Methylated lysine 79 of histone H3 targets 53BP1 to DNA double-strand breaks. *Nature* **432**, 406–411
25. Schulze, J. M., Jackson, J., Nakanishi, S., Gardner, J. M., Hentrich, T., Haug, J., Johnston, M., Jaspersen, S. L., Kobor, M. S., and Shilatifard, A. (2009) Linking cell cycle to histone modifications: SBF and H2B monoubiquitination machinery and cell-cycle regulation of H3K79 dimethylation. *Mol. Cell* **35**, 626–641
26. Shanower, G. A., Muller, M., Blanton, J. L., Honti, V., Gyurkovics, H., and Schedl, P. (2005) Characterization of the grappa gene, the *Drosophila* histone H3 lysine 79 methyltransferase. *Genetics* **169**, 173–184
27. Ooga, M., Inoue, A., Kageyama, S., Akiyama, T., Nagata, M., and Aoki, F. (2008) Changes in H3K79 methylation during preimplantation development in mice. *Biol. Reprod.* **78**, 413–424
28. Bitoun, E., Oliver, P. L., and Davies, K. E. (2007) The mixed-lineage leukemia fusion partner AF4 stimulates RNA polymerase II transcriptional elongation and mediates coordinated chromatin remodeling. *Hum. Mol. Genet.* **16**, 92–106
29. Mueller, D., Bach, C., Zeisig, D., Garcia-Cuellar, M. P., Monroe, S., Sreekumar, A., Zhou, R., Nesvizhskii, A., Chinnaiyan, A., Hess, J. L., and Slany, R. K. (2007) A role for the MLL fusion partner ENL in transcriptional elongation and chromatin modification. *Blood* **110**, 4445–4454
30. Bernt, K. M., Zhu, N., Sinha, A. U., Vempati, S., Faber, J., Krivtsov, A. V., Feng, Z., Punt, N., Daigle, A., Bullinger, L., Pollock, R. M., Richon, V. M., Kung, A. L., and Armstrong, S. A. (2011) MLL-rearranged leukemia is dependent on aberrant H3K79 methylation by DOT1L. *Cancer Cell* **20**, 66–78
31. Frescas, D., Guardavaccaro, D., Bassermann, F., Koyama-Nasu, R., and Pagano, M. (2007) JHDM1B/FBXL10 is a nucleolar protein that represses transcription of ribosomal RNA genes. *Nature* **450**, 309–313
32. Tsukada, Y., Fang, J., Erdjument-Bromage, H., Warren, M. E., Borchers, C. H., Tempst, P., and Zhang, Y. (2006) Histone demethylation by a family of JmjC domain-containing proteins. *Nature* **439**, 811–816
33. Wang, T., Chen, K., Zeng, X., Yang, J., Wu, Y., Shi, X., Qin, B., Zeng, L., Esteban, M. A., Pan, G., and Pei, D. (2011) The histone demethylases Jhdm1a/1b enhance somatic cell reprogramming in a vitamin-C-dependent manner. *Cell Stem Cell* **9**, 575–587
34. Wu, X., Johansen, J. V., and Helin, K. (2013) Fbxl10/Kdm2b recruits polycomb repressive complex 1 to CpG islands and regulates H2A ubiquitylation. *Mol. Cell* **49**, 1134–1146
35. Farcas, A. M., Blackledge, N. P., Sudbery, I., Long, H. K., McGouran, J. F., Rose, N. R., Lee, S., Sims, D., Cerase, A., Sheahan, T. W., Koseki, H., Brockdorff, N., Ponting, C. P., Kessler, B. M., and Klose, R. J. (2012) KDM2B links the polycomb repressive complex 1 (PRC1) to recognition of CpG islands. *eLife* **1**, e00205
36. Blackledge, N. P., Farcas, A. M., Kondo, T., King, H. W., McGouran, J. F., Hanssen, L. L., Ito, S., Cooper, S., Kondo, K., Koseki, Y., Ishikura, T., Long, H. K., Sheahan, T. W., Brockdorff, N., Kessler, B. M., Koseki, H., and Klose, R. J. (2014) Variant PRC1 complex-dependent H2A ubiquitylation drives PRC2 recruitment and polycomb domain formation. *Cell* **157**, 1445–1459
37. He, J., Shen, L., Wan, M., Taranova, O., Wu, H., and Zhang, Y. (2013) Kdm2b maintains murine embryonic stem cell status by recruiting PRC1 complex to CpG islands of developmental genes. *Nat. Cell Biol.* **15**, 373–384
38. Liang, G., He, J., and Zhang, Y. (2012) Kdm2b promotes induced pluripotent stem cell generation by facilitating gene activation early in reprogramming. *Nat. Cell Biol.* **14**, 457–466
39. Tzatsos, A., Pfau, R., Kampranis, S. C., and Tsichlis, P. N. (2009) Ndy1/KDM2B immortalizes mouse embryonic fibroblasts by repressing the Ink4a/Arf locus. *Proc. Natl. Acad. Sci. USA* **106**, 2641–2646
40. Pfau, R., Tzatsos, A., Kampranis, S. C., Serebrennikova, O. B., Bear, S. E., and Tsichlis, P. N. (2008) Members of a family of JmjC domain-containing oncoproteins immortalize embryonic fibroblasts *via* a JmjC domain-dependent process. *Proc. Natl. Acad. Sci. USA* **105**, 1907–1912
41. Tzatsos, A., Paskaleva, P., Ferrari, F., Deshpande, V., Stoykova, S., Contino, G., Wong, K. K., Lan, F., Trojer, P., Park, P. J., and Bardeesy, N. (2013) KDM2B promotes pancreatic cancer *via* polycomb-dependent and -independent transcriptional programs. *J. Clin. Invest.* **123**, 727–739
42. He, J., Nguyen, A. T., and Zhang, Y. (2011) KDM2b/JHDM1b, an H3K36me2-specific demethylase, is required for initiation and maintenance of acute myeloid leukemia. *Blood* **117**, 3869–3880
43. Jia, G., Wang, W., Li, H., Mao, Z., Cai, G., Sun, J., Wu, H., Xu, M., Yang, P., Yuan, W., Chen, S., and Zhu, B. (2009) A systematic evaluation of the compatibility of histones containing methyl-lysine analogues with biochemical reactions. *Cell Res.* **19**, 1217–1220
44. Simon, M. D., Chu, F., Racki, L. R., de la Cruz, C. C., Burlingame, A. L., Panning, B., Narlikar, G. J., and Shokat, K. M. (2007) The site-specific installation of methyl-lysine analogs into recombinant histones. *Cell* **128**, 1003–1012
45. Lizcano, J. M., Unzeta, M., and Tipton, K. F. (2000) A spectrophotometric method for determining the oxidative deamination of methylamine by the amine oxidases. *Anal. Biochem.* **286**, 75–79
46. Gil, J., and O'Loghlen, A. (2014) PRC1 complex diversity: where is it taking us? *Trends Cell Biol.* **24**, 632–641
47. Di Croce, L., and Helin, K. (2013) Transcriptional regulation by polycomb group proteins. *Nat. Struct. Mol. Biol.* **20**, 1147–1155
48. Sánchez, C., Sánchez, I., Demmers, J. A., Rodriguez, P., Strouboulis, J., and Vidal, M. (2007) Proteomics analysis of Ring1B/Rnf2 interactors identifies a novel complex with the Fbxl10/Jhdm1B histone demethylase and the Bcl6 interacting corepressor. *Mol. Cell. Proteomics* **6**, 820–834
49. Béguelin, W., Teater, M., Gearhart, M. D., Calvo Fernández, M. T., Goldstein, R. L., Cárdenas, M. G., Hatzi, K., Rosen, M., Shen, H., Corcoran, C. M., Hamline, M. Y., Gascoyne, R. D., Levine, R. L., Abdel-Wahab, O., Licht, J. D., Shaknovich, R., Elemento, O., Bardwell, V. J., and Melnick, A. M. (2016) EZH2 and BCL6 cooperate to assemble CBX8-BCOR complex to repress bivalent promoters, mediate germinal center formation and lymphomagenesis. *Cancer Cell* **30**, 197–213
50. Shi, Y., Lan, F., Matson, C., Mulligan, P., Whetstine, J. R., Cole, P. A., Casero, R. A., and Shi, Y. (2004) Histone demethylation mediated by the nuclear amine oxidase homolog LSD1. *Cell* **119**, 941–953
51. Cheng, Z., Cheung, P., Kuo, A. J., Yukl, E. T., Wilmot, C. M., Gozani, O., and Patel, D. J. (2014) A molecular threading mechanism underlies Jumonji lysine demethylase KDM2A regulation of methylated H3K36. *Genes Dev.* **28**, 1758–1771

52. Bracken, A. P., Dietrich, N., Pasini, D., Hansen, K. H., and Helin, K. (2006) Genome-wide mapping of polycomb target genes unravels their roles in cell fate transitions. *Genes Dev.* **20**, 1123–1136
53. Van den Boom, V., Maat, H., Geugien, M., Rodríguez López, A., Sotoca, A. M., Jaques, J., Brouwers-Vos, A. Z., Fusetti, F., Groen, R. W., Yuan, H., Martens, A. C., Stunnenberg, H. G., Vellenga, E., Martens, J. H., and Schuringa, J. J. (2016) Non-canonical PRC1.1 targets active genes independent of H3K27me3 and is essential for leukemogenesis. *Cell Reports* **14**, 332–346
54. Ng, H. H., Feng, Q., Wang, H., Erdjument-Bromage, H., Tempst, P., Zhang, Y., and Struhl, K. (2002) Lysine methylation within the globular domain of histone H3 by Dot1 is important for telomeric silencing and Sir protein association. *Genes Dev.* **16**, 1518–1527
55. Vaquero, A., Scher, M., Lee, D., Erdjument-Bromage, H., Tempst, P., and Reinberg, D. (2004) Human SirT1 interacts with histone H1 and promotes formation of facultative heterochromatin. *Mol. Cell* **16**, 93–105
56. Gilan, O., Lam, E. Y., Becher, I., Lugo, D., Cannizzaro, E., Joberty, G., Ward, A., Wiese, M., Fong, C. Y., Ftouni, S., Tyler, D., Stanley, K., MacPherson, L., Weng, C. F., Chan, Y. C., Ghisi, M., Smil, D., Carpenter, C., Brown, P., Garton, N., Blewitt, M. E., Bannister, A. J., Kouzarides, T., Huntly, B. J., Johnstone, R. W., Drewes, G., Dawson, S. J., Arrowsmith, C. H., Grandi, P., Prinjha, R. K., and Dawson, M. A. (2016) Functional interdependence of BRD4 and DOT1L in MLL leukemia. *Nat. Struct. Mol. Biol.* **23**, 673–681
57. Chen, C. W., Koche, R. P., Sinha, A. U., Deshpande, A. J., Zhu, N., Eng, R., Doench, J. G., Xu, H., Chu, S. H., Qi, J., Wang, X., Delaney, C., Bernt, K. M., Root, D. E., Hahn, W. C., Bradner, J. E., and Armstrong, S. A. (2015) DOT1L inhibits SIRT1-mediated epigenetic silencing to maintain leukemic gene expression in MLL-rearranged leukemia. *Nat. Med.* **21**, 335–343
58. Mersfelder, E. L., and Parthun, M. R. (2006) The tale beyond the tail: histone core domain modifications and the regulation of chromatin structure. *Nucleic Acids Res.* **34**, 2653–2662
59. Tan, J., Jones, M., Koseki, H., Nakayama, M., Muntean, A. G., Maillard, I., and Hess, J. L. (2011) CBX8, a polycomb group protein, is essential for MLL-AF9-induced leukemogenesis. *Cancer Cell* **20**, 563–575
60. Blackledge, N. P., Zhou, J. C., Tolstorukov, M. Y., Farcas, A. M., Park, P. J., and Klose, R. J. (2010) CpG islands recruit a histone H3 lysine 36 demethylase. *Mol. Cell* **38**, 179–190
61. Hong, S., Cho, Y. W., Yu, L. R., Yu, H., Veenstra, T. D., and Ge, K. (2007) Identification of JmjC domain-containing UTX and JMJD3 as histone H3 lysine 27 demethylases. *Proc. Natl. Acad. Sci. USA* **104**, 18439–18444
62. Agger, K., Cloos, P. A., Christensen, J., Pasini, D., Rose, S., Rappsilber, J., Issaeva, I., Canaani, E., Salcini, A. E., and Helin, K. (2007) UTX and JMJD3 are histone H3K27 demethylases involved in HOX gene regulation and development. *Nature* **449**, 731–734
63. Im, H., Park, C., Feng, Q., Johnson, K. D., Kiekhaefer, C. M., Choi, K., Zhang, Y., and Bresnick, E. H. (2003) Dynamic regulation of histone H3 methylated at lysine 79 within a tissue-specific chromatin domain. *J. Biol. Chem.* **278**, 18346–18352
64. Pokholok, D. K., Harbison, C. T., Levine, S., Cole, M., Hannett, N. M., Lee, T. I., Bell, G. W., Walker, K., Rolfe, P. A., Herbolsheimer, E., Zeitlinger, J., Lewitter, F., Gifford, D. K., and Young, R. A. (2005) Genome-wide map of nucleosome acetylation and methylation in yeast. *Cell* **122**, 517–527
65. Altaf, M., Utley, R. T., Lacoste, N., Tan, S., Briggs, S. D., and Côté, J. (2007) Interplay of chromatin modifiers on a short basic patch of histone H4 tail defines the boundary of telomeric heterochromatin. *Mol. Cell* **28**, 1002–1014
66. Millar, C. B., Kurdistani, S. K., and Grunstein, M. (2004) Acetylation of yeast histone H4 lysine 16: a switch for protein interactions in heterochromatin and euchromatin. *Cold Spring Harb. Symp. Quant. Biol.* **69**, 193–200
67. Lenstra, T. L., Benschop, J. J., Kim, T., Schulze, J. M., Brabers, N. A., Margaritis, T., van de Pasch, L. A., van Heesch, S. A., Brok, M. O., Groot Koerkamp, M. J., Ko, C. W., van Leenen, D., Sameith, K., van Hooff, S. R., Lijnzaad, P., Kemmeren, P., Hentrich, T., Kobor, M. S., Buratowski, S., and Holstege, F. C. (2011) The specificity and topology of chromatin interaction pathways in yeast. *Mol. Cell* **42**, 536–549
68. Lee, S. H., Um, S. J., and Kim, E. J. (2013) CBX8 suppresses Sirtinol-induced premature senescence in human breast cancer cells *via* co-operation with SIRT1. *Cancer Lett.* **335**, 397–403
69. Yuan, W., Xu, M., Huang, C., Liu, N., Chen, S., and Zhu, B. (2011) H3K36 methylation antagonizes PRC2-mediated H3K27 methylation. *J. Biol. Chem.* **286**, 7983–7989

Received for publication February 5, 2018.
Accepted for publication April 30, 2018.